Characterization of the Role of Polar Amino Acid Residues within Predicted Transmembrane Helix 17 in Determining the Substrate Specificity of Multidrug Resistance Protein 3†

Da-Wei Zhang,[‡,§] Hong-Mei Gu,[||] Monika Vasa,[‡] Mario Muredda,[‡,⊥] Susan P. C. Cole,[‡,§] and Roger G. Deeley*[,‡,§,⊥]

Division of Cancer Biology and Genetics, Cancer Research Institute, and Departments of Pathology, Biochemistry, and Anatomy and Cell Biology, Queen's University, Kingston, Ontario K7L 3N6, Canada

Received March 21, 2003; Revised Manuscript Received May 29, 2003

ABSTRACT: Human multidrug resistance protein (MRP) 3 is the most closely related homologue of MRP1. Like MRP1, MRP3 confers resistance to etoposide (VP-16) and actively transports 17β-estradiol 17-(β-D-glucuronide) ($E_2$17βG), cysteinyl leukotriene 4 (LTC_4), and methotrexate, although with generally lower affinity. Unlike MRP1, MRP3 also transports monovalent bile salts. We have previously demonstrated that hydrogen-bonding residues predicted to be in the inner-leaflet spanning segment of transmembrane (TM) 17 of MRP1 are important for drug resistance and $E_2$17βG transport. We have now examined the importance of the hydrogen-bonding potential of residues in TM17 of MRP3 on both substrate specificity and overall activity. Mutation S1229A reduced only methotrexate transport. Mutations S1231A and N1241A decreased resistance to VP-16 and transport of $E_2$17βG and methotrexate but not taurocholate. Mutation Q1235A also reduced resistance to VP-16 and transport of $E_2$17βG but increased taurocholate transport without affecting transport of methotrexate. Mutations Y1232F and S1233A reduced resistance to VP-16 and the transport of all three substrates tested. In contrast, mutation T1237A markedly increased VP-16 resistance and transport of all substrates. On the basis of the substrates analyzed, residues Ser^{1229}, Ser^{1231}, Gln^{1235}, and Asn^{1241} play an important role in determining the specificity of MRP3, while mutation of Tyr^{1232}, Ser^{1233}, and Thr^{1237} affects overall activity. Unlike MRP1, the involvement of polar residues in determining substrate specificity extends throughout the TM helix. Furthermore, elimination of the hydrogen-bonding potential of a single amino acid, Thr^{1237}, markedly enhanced the ability of the protein to confer drug resistance and to transport all substrates examined.

The frequent occurrence of resistance to a wide variety of structurally and functionally unrelated anticancer drugs is a significant barrier to successful treatment of cancer patients. Experimentally and in some cases clinically, multidrug resistance (MDR)[1] is often associated with overexpression of ATP-dependent drug-efflux pumps, such as multidrug resistance protein 1 (MRP1), P-glycoprotein (P-gp), and breast cancer resistance protein (BCRP/MXR), all of which belong to the ATP binding cassette (ABC) superfamily of transporters (*1*−*10*). MRP1, or ABCC1, is a member of the ABCC branch of the superfamily and can confer resistance to many commonly used, structurally diverse natural product chemotherapeutic agents, including anthracyclines, *Vinca* alkaloids, and epipodophyllotoxins (*11*−*14*). The protein is also a primary active transporter of many glutathione-, glucuronate-, and sulfate-conjugated organic anions (*15*−*19*).

Since the identification of MRP1, several MRP1-related proteins have been cloned, including MRP2 to -7 and ABCC11 and -12 (*20*−*29*). Among the MRP family members, MRP3 shares the highest degree of structural resemblance to MRP1 (58% amino acid identity). MRP3, which is composed of 1527 amino acid residues, is predicted to contain a typical ABC transporter core structure, consisting of two membrane-spanning domains (MSDs) and two nucleotide binding domains, plus an additional NH_2-terminal MSD (MSD1) that is comprised of five transmembrane (TM) helices (*24*). Thus, the predicted topology of MRP3 is similar to that of MRP1 (*30*−*33*), containing a total of 17 TM helices with an extracellular NH_2 terminus.

† This work was supported by a grant from the National Cancer Institute of Canada with funds from the Terry Fox Run. D.-W.Z. was supported in part by a Queen's University Graduate Award. S.P.C.C. is a Canada Research Chair in Cancer Biology and Senior Scientist of Cancer Care Ontario. R.G.D. is a Stauffer Research Professor of Queen's University and Vice President of Research Cancer Care Ontario.

* To whom correspondence should be addressed at Cancer Research Laboratories, Botterell Hall, Queen's University, Kingston, Ontario K7L 3N6, Canada. Tel: 613-533-2979. Fax: 613-533-6830. E-mail: deeleyr@post.queensu.ca.

‡ Division of Cancer Biology and Genetics, Cancer Research Institute, Queen's University.

§ Department of Pathology, Queen's University.

|| Department of Anatomy and Cell Biology, Queen's University.

⊥ Department of Biochemistry, Queen's University.

[1] Abbreviations: MDR, multidrug resistance; MRP, multidrug resistance protein; P-gp, P-glycoprotein; BCRP/MXR, breast cancer resistance protein; MSD, membrane-spanning domain; TM, transmembrane; NBD, nucleotide binding domain; mAb, monoclonal antibody; VP-16, etoposide; $E_2$17β, 17β-estradiol 17-(β-D-glucuronide); LTC_4, leukotriene C_4; MTT, 3-(4,5-dimethylthiazol-2-yl)-2,5-diphenyltetrazolium bromide; PBS, phosphate-buffered saline; SDS−PAGE, sodium dodecyl sulfate−polyacrylamide gel electrophoresis; HEK, human embryonic kidney; MTX, methotrexate; TC, taurocholate.

10.1021/bi034462b CCC: $25.00
Published on Web 08/02/2003

Several studies using transfected cells have demonstrated that, when overexpressed, MRP3 increases resistance to etoposide (VP-16) (*34*, *35*). MRP3 is also capable of transporting methotrexate in an ATP-dependent manner and conferring a high level of resistance to short-term exposure to this drug (*36*−*38*). Increased expression of MRP3 has also been observed in some solid tumors (*39*−*43*). One study reported that plasma membrane expression of MRP2 and MRP3, but not MRP1, could contribute to the MDR phenotype in human hepatocellular carcinoma (*41*). In addition, membrane vesicles prepared from MRP3-transfected cells transport the MRP1 and MRP2 substrates 17β-estradiol 17-(β-D-glucuronide) ($E_2$17βG), cysteinyl leukotriene 4 (LTC_4), and dinitrophenyl-*S*-glutathione (*35*, *37*, *38*, *44*). However, LTC_4 is a low-affinity substrate of MRP3 (K_m ~5.0 μM), in comparison to MRP1 (K_m ~0.1 μM) and MRP2 (K_m ~1.0 μM). In addition to methotrexate, MRP3 also actively transports folic acid and leucovorin (*36*). Among the substrate specificity differences from MRP1, one of the most striking is MRP3's ability to transport conjugated monoanionic bile acids such as taurocholic and glycocholic acids (*38*, *45*−*48*).

The physiological functions of MRP3 remain largely unknown. The protein is present in adrenal gland, kidney, ileum, colon, pancreas, and gall bladder and at relatively low levels in normal liver (*42*, *49*−*51*). Like MRP1, MRP3 is localized in basolateral membranes (*49*, *51*−*53*). It has been reported that expression of MRP3 in human enterocytes was increased by bile salts (*54*), suggesting a role for MRP3 in the enterohepatic circulation of bile salts by transporting them from enterocytes into the circulation and so preventing the accumulation of intracellular bile salts. The hepatic expression of MRP3 was also significantly enhanced in rats made cholestatic by bile duct ligation and in humans suffering from cholestasis (*52*, *55*−*57*). These findings suggest a role for MRP3 in the removal of organic anions from the liver into the blood under cholestatic conditions.

In the present study, we initially characterized the drug resistance and transport profiles of wild-type MRP3 in human embryonic kidney (HEK293) cells stably overexpressing the protein. These studies confirmed that MRP3 was capable of increasing resistance to VP-16 but not to doxorubicin, cisplatin, and vincristine and of transporting $E_2$17βG and methotrexate. We also found that human MRP3 transported taurocholate in an ATP-dependent manner. How MRP3 recognizes these structurally diverse substrates is unclear. Identification of specific amino acid residues in MRP3 involved in overall function and/or substrate specificity is at a very early stage (*48*, *58*). We previously demonstrated that mutations of certain amino acid residues with side chains capable of hydrogen bonding within TM17 of MRP1 can modulate substrate specificity of the protein (*59*−*61*). In addition, we have recently shown that mutations of a highly conserved tryptophan predicted to be at or close to the cytoplasmic membrane interface of TM17 in both MRP1 and MRP3 have different effects on the substrate specificities of the two proteins (*48*, *61*). The whole of TM17 is exceptionally well conserved between MRP3 (residues 1224−1244) and MRP1 (residues 1228−1248) with 19 of 21 amino acids being identical. Given the overlapping but nevertheless distinct substrate specificities of MRP1 and MRP3, we have now investigated the role of all other polar residues within TM17 in determining the substrate specificity of MRP3. The mutant proteins have been stably expressed in HEK293 cells and the transfectants characterized with respect to their ability to confer VP-16 resistance and to transport methotrexate, $E_2$17βG, and taurocholate. The results of these studies demonstrated that all polar residues, predicted to be in TM17 of MRP3, affected the substrate specificity and/or overall activity of the protein to varying extents. The data also indicate that despite the highly conserved structure of TM17, MRP1 and MRP3 display major differences with respect to the interaction of both conserved and nonconserved amino acid residues in TM17 with common substrates.

EXPERIMENTAL PROCEDURES

Materials. Culture medium and fetal bovine serum were obtained from Invitrogen. [^{3}H]$E_2$17βG (44 Ci/mmol) and [^{3}H]taurocholate (2 Ci/mmol) were from Perkin-Elmer Life Sciences, and [^{3}H]methotrexate (29 Ci/mmol) was from Moravek Biochemicals, Inc. (Brea, CA). Doxorubicin hydrochloride, etoposide (VP-16), and vincristine sulfate were obtained from Sigma.

Site-Directed Mutagenesis. Full-length MRP3 cDNA with an optimized Kozak sequence was generated by reverse transcriptase PCR using mRNA from the human non small cell lung cancer cell line A549. The MRP3 cDNA was introduced into pBluescript II KS$^+$ (Stratagene, La Jolla, CA) and sequenced. The sequence obtained was identical to that published previously (accession no. CAA76658; gi 3087794). All mutations were generated using the Transformer site-directed mutagenesis kit (CLONTECH). Templates were prepared by cloning ~1.6 kb restriction fragments of human MRP3 nucleotides into pGEM-3Zf (Promega). Mutagenesis was then performed according to the manufacturer's instructions using a selection primer 5′-GAG AGT GCA CGA TAT CCG GTG TG-3′ that mutates a unique *Nde*I site in the vector to an *Eco*RV restriction site. Oligonucleotides bearing mismatched bases at the residues to be mutated (underlined) were synthesized by ACGT Corp. (Toronto, Canada). They are as follows: S1229A (5′-GGG CTG GTG GGG CTA GCT GTG TCC TAC TCC-3′), S1231A (5′-GC CTT TCT GTG GCC TAC TCC CTG CAG GTG ACA-3′), Y1232F (5′-T TCT GTG TCC TTC TCC TTA CAG GTG ACA TTT G-3′), S1233A (5′-CT GTG TCC TAC GCC CTG CAG GTG ACA TTT G-3′), Q1235A (5′-G TCC TAC TCC TTG GCG GTG ACA TTT GCT C-3′), T1237A (5′-CC TTG CAG GTG GCA TTC GCT CTG AAC TGG-3′), T1237S (5′-CC TTG CAG GTG TCC TTC GCT CTG AAC TGG-3′), T1237G (5′-CC TTG CAG GTG GGA TTC GCT CTG AAC TGG-3′), T1237L (5′-CC TTG CAG GTG CTA TTC GCT CTG AAC TGG-3′), and N1241A (5′-GTG ACA TTT GCG CTA GCC TGG ATG ATA C-3′).

All mutations were confirmed by sequencing using DNA thermo sequenase and Cy5.5 and Cy5.0 dye terminator/primer (Amersham Biosciences). DNA fragments containing the desired mutations were transferred into pCEBV7-MRP3, after which the entire mutated inserts and the cloning sites were verified by DNA sequencing (ACGT Corp., Toronto, Canada).

Cell Lines and Tissue Culture. All of the wild-type and mutated MRP3 constructs were analyzed as stably transfected HEK293 cells grown in DMEM supplemented with 10%

fatal bovine serum and 100 μg/mL hygromycin B (Roche) as described previously (*13*, *62*). Briefly, HEK293 cells were transfected with pCEBV7 vectors containing wild-type or mutant MRP3 using Fugene6 (Roche Molecular Biochemicals) according to the manufacturer's instructions. After ~48 h, the transfected cells were supplemented with fresh medium containing 100 μg/mL hygromycin B. Approximately 3 weeks posttransfection, the hygromycin B-resistant cells were cloned by limiting dilution, and the resulting cell lines were tested for expression of the wild-type and mutant proteins.

Determination of Protein Levels in Transfected Cells. Plasma membrane vesicles were prepared by centrifugation through sucrose, as described previously (*15*, *16*). After determination of protein levels by Bradford assay (Bio-Rad), total membrane protein (0.5, 1.0, and 1.25 μg) from transfectants expressing wild-type MRP3 and various mutant proteins were analyzed by sodium dodecyl sulfate−polyacrylamide gel electrophoresis using a 7.5% gel. Proteins were subsequently transferred to Immobilon-P poly(vinylidene difluoride) membranes (Millipore, Bedford, MA) by electroblotting. The proteins were detected with monoclonal antibody (mAb), M3II-9 (Kamiya Biomedical Co., Seattle, WA). Antibody binding was detected with horseradish peroxidase-conjugated goat anti-mouse IgG (Pierce), followed by enhanced chemiluminescence detection and X-Omat Blue XB-1 films (Perkin-Elmer Life Sciences). Densitometry of the film images was performed using a ChemiImager 4000 (Alpha Innotech Corp., San Leandro, CA). The relative protein expression levels were calculated by dividing the integrated densitometry values obtained for 0.5, 1.0, and 1.25 μg of total membrane protein from transfectants expressing the mutant proteins by the integrated densitometry values obtained for the comparable amounts of total membrane proteins from transfectants expressing the wild-type protein. Each comparison was performed at least three times in independent experiments. The results were then pooled, and the mean values were used for normalization purposes.

Chemosensitivity Testing. Drug resistance was determined using the colorimetric 3-(4,5-dimethylthiazol-2-yl)-2,5-diphenyltetrazolium bromide (MTT) assay as described previously (*11*, *13*, *59*, *60*, *62*). Briefly, cells were seeded at 7×10^3 cells/well in 100 μL of culture medium in 96-well tissue culture plates. The following day, various concentrations of drug diluted in culture medium were added to cells (100 μL/well). After incubation for an additional 96 h, 100 μL of medium was removed from each well, and the MTT reagent [25 μL/well, 2 mg/mL phosphate-buffered saline (PBS)] (Sigma) was added. After 3 h, the formazan was solubilized by mixing with 1 N HCl/isopropyl alcohol (1:24) (100 μL/well). Color density was determined using the ELX 800 UV spectrophotometer (570 nm). Mean values of quadruplicate determinations ± SD were plotted using GraphPad software. IC_{50} values were obtained from the best fit of the data to a sigmoidal curve. Relative resistance is expressed as the ratio of the IC_{50} value of cells transfected with MRP3 expression vectors to that of cells transfected with empty vector. Resistance factors were determined in three or more independent experiments. The significance of the difference between relative resistance factors of wild-type and mutant MRP3 transfectants was determined using an unpaired Student's *t* test.

$E_2$17βG, Taurocholate, and Methotrexate Transport by Membrane Vesicles. Plasma membrane vesicles were prepared as described previously, and ATP-dependent transport of [^{3}H]$E_2$17βG into the inside-out membrane vesicles was measured by a rapid filtration technique (*15*, *16*). Briefly, vesicles (20 μg of total proteins) were incubated at 37 °C in 100 μL of transport buffer (50 mM Tris-HCl, 250 mM sucrose, 0.02% sodium azide, pH 7.4) containing ATP or AMP (4 mM), 10 mM $MgCl_2$, and [^{3}H]$E_2$17βG (400 nM, 100 nCi). At the indicated times, 20 μL aliquots were removed and added to 1 mL of ice-cold transport buffer, followed by filtration under vacuum through glass fiber filters (Type A/E, Gelman Sciences, Dorval, Quebec, Canada). Filters were immediately washed twice with 4 mL of cold transport buffer, and the bound radioactivity was determined by scintillation counting. All data were corrected for the amount of [^{3}H]$E_2$17βG that remained bound to the filter in the absence of vesicle protein (usually <5% of the total radioactivity). [^{3}H]$E_2$17βG uptake was expressed relative to the total protein concentration in each reaction. ATP-dependent uptake of [^{3}H]taurocholate (4 μM) and [^{3}H]-methotrexate (1 μM) was measured as described for [^{3}H]E_2-17βG. Glass fiber filters used for examining [^{3}H]taurocholate uptake were soaked in transport buffer containing methylated bovine albumin (Sigma, 1 mg/mL) overnight at 4 °C.

K_m and V_{max} values of ATP-dependent [^{3}H]taurocholate uptake by membrane vesicles (5 μg of total proteins) were measured at various taurocholate concentrations (1−32 μM) for 5 min at 37 °C in 25 μL of transport buffer containing 4 mM ATP and 10 mM $MgCl_2$, followed by nonlinear regression analyses. Kinetic parameters of ATP-dependent [^{3}H]$E_2$17βG (0.1−135 μM) uptake were determined as described for [^{3}H]taurocholate except that the reaction was carried out for 1 min at 37 °C.

RESULTS

Characterization of Wild-Type MRP3 in Stably Transfected HEK293 Cells. The episomal expression vector, pCEBV7, containing the wild-type form of MRP3 cDNA was used to stably transfect HEK293 cells, and populations of transfected cells were selected in hygromycin B. The resultant stably transfected cell populations were cloned by limiting dilution, and subpopulations expressing high levels of MRP3 were used in subsequent studies. Immunoblot analysis of plasma membrane vesicles isolated from MRP3 stably transfected HEK293 cells revealed an intensely immunoreactive M_r 190000 band after reaction with mAb, M3II-9 (Figure 1A). The expression level of MRP3 proteins was comparable to that of wild-type MRP1 in previously characterized HEK stable transfectants (*13*), as determined by normalization of the levels of both proteins using MRP1/MRP3 hybrids as standards for immunoblotting (data not shown). Endogenous MRP3 in HEK293 cells transfected with the empty vector was undetectable under the conditions used (Figure 1A). The relative resistance of transfectants expressing wild-type MRP3 was determined by MTT assays following exposure to various concentrations of vincristine, doxorubicin, cisplatin, and VP-16 (Figure 1). We could not detect any significant resistance to cisplatin, doxorubicin, and vincristine in MRP3 stably transfected HEK293 cells (Figure 1B−D). In contrast, cells stably expressing MRP3 showed significant resistance to VP-16 when compared with cells transfected

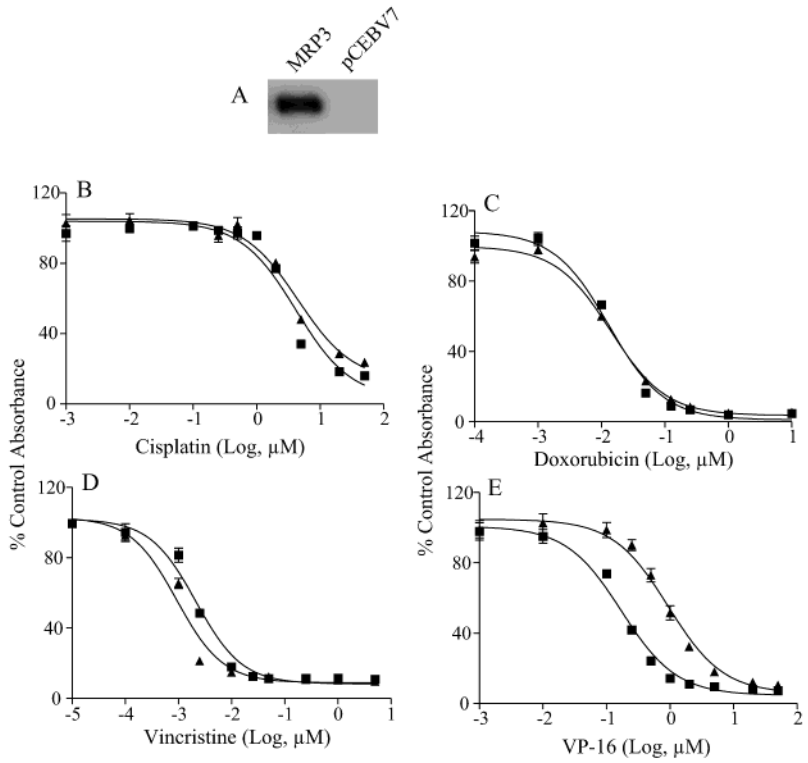

FIGURE 1: Resistance of stably transfected HEK293 cells to cisplatin (B), doxorubicin (C), vincristine (D), and VP-16 (E). Expression levels of MRP3 protein in stably transfected HEK293 cells used for MTT assays were determined by immunoblotting of membrane vesicle preparations as described. Blots (panel A) were probed with the MRP3-specific mAb M3II-9. The relative resistance of cells expressing wild-type human MRP3 ($HEK293_{MRP3}$, ▲) and cells transfected with the empty expression vector ($HEK293_{pC7}$, ■) was determined as described.

with empty vector (Figure 1E), consistent with previous studies (*34*, *35*). Under the same conditions, we examined the drug resistance profile of previously described HEK transfectants expressing wild-type MRP1 (data not shown) (*13*). As previously reported, MRP1 conferred significant resistance to VP-16 but not to cisplatin. However, unlike MRP3 transfectants, cells stably expressing MRP1 also showed high and moderate levels of resistance to both vincristine and doxorubicin. The relative levels of resistance to vincrinstine and doxorubicin conferred by MRP1 were approximately 20- and 6-fold, respectively, when compared with the control transfectants, consistent with previous studies (*13*, *59*, *60*, *62*).

Membrane vesicles enriched in MRP3 have been demonstrated to transport $E_2 17\beta G$ and LTC_4, as well as methotrexate and conjugated monoanionic bile acid glycocholate (*35*, *37*, *38*, *44*). Using a transient transfection system, we found previously that human MRP3 also transported another monovalent bile salt, taurocholate (*48*). In this study, we have confirmed the observation using stable HEK293 transfectants (Figure 2A) and defined the kinetic parameters of taurocholate transport (Figure 2B). Nonlinear regression analysis of the data yielded apparent K_m and V_{max} values of 30 ± 9 μM and 464 ± 84 pmol mg^{-1} $(5\ min)^{-1}$. Moreover, transport of the common MRP1, MRP2, and MRP3 substrate, $E_2 17\beta G$, was inhibited by taurocholate with an IC_{50} value of approximately 40 μM (Figure 2C). Under the same conditions, membrane vesicles prepared from MRP1 stably transfected HEK293 cells did not showed any ATP-dependent [^{3}H]-taurocholate uptake when compared with membrane vesicles isolated from the control cells transfected with the empty vector (data not shown).

Effect of Mutations on MRP3-Mediated [^{3}H]$E_2 17\beta G$, [^{3}H]-Methotrexate, and [^{3}H]Taurocholate Transport. We have previously shown that several polar residues within TM17 of MRP1, as well as the highly conserved Trp^{1242} in TM17 of MRP3, play important roles in the overall activity and/or substrate specificity of these proteins (*48*, *59*−*60*). To examine the functional importance of all remaining polar residues in TM17 of MRP3, we generated a series of seven mutant proteins in which Ser^{1229}, Ser^{1231}, Ser^{1233}, Gln^{1235}, Thr^{1237}, or Asn^{1241} was replaced with Ala and Tyr^{1232} was substituted with Phe (Figure 3). These mutant proteins were then stably expressed in HEK293 cells so that the effects of the mutations on both the transport of known substrates and the ability of the protein to confer drug resistance could be determined.

Stably transfected cell populations expressing high levels of MRP3 mutant proteins were isolated as described for wild-type MRP3, and the levels of mutant proteins relative to that of wild-type MRP3 were determined by immunoblotting and densitometry, as described. The expression levels of the mutant proteins in stably transfected HEK293 cells were similar to that of wild-type MRP3 (Figure 4A). The effects of the mutations on the transport of $E_2 17\beta G$ were then determined by transport assays (Figure 4B−E). Replacement of Ser^{1229} with Ala had no significant effect on MRP3-mediated $E_2 17\beta G$ uptake, whereas mutations S1231A, Y1232F, S1233A, Q1235A, and N1241A all decreased the transport activity. In contrast, conversion of Thr^{1237} to Ala resulted in a significant (∼2.0-fold) increase in transport activity.

We next examined the effect of mutations on methotrexate transport (Figure 5). Replacement of Gln^{1235} by Ala had no

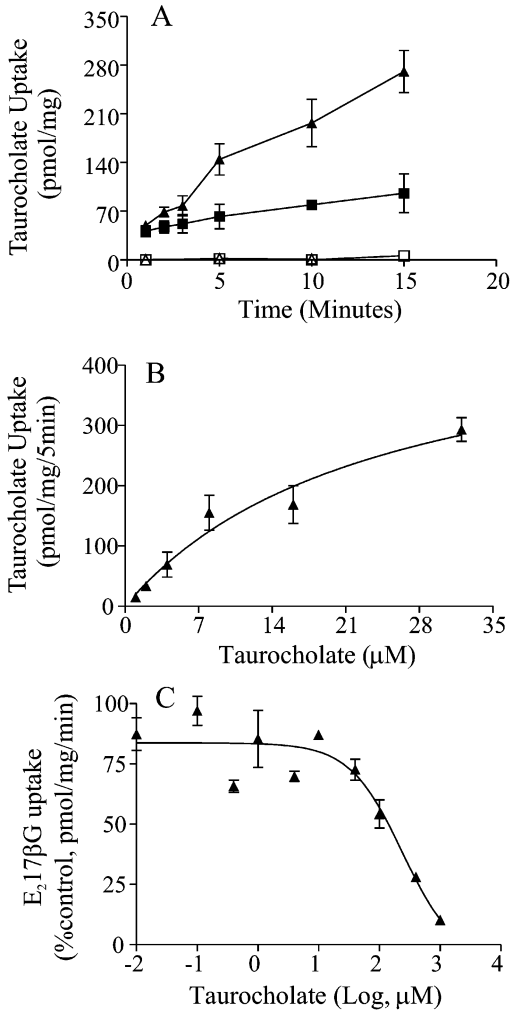

FIGURE 2: Transport of taurocholate by MRP3. Panel A: Time course of ATP-dependent [^{3}H]taurocholate uptake by membrane vesicles prepared from HEK293 stable transfectant expressing wild-type MRP3. Membrane vesicles were incubated at 37 °C with 4 μM [^{3}H]taurocholate in transport buffer for the time indicated, as described. Panel B: Kinetics of ATP-dependent [^{3}H]taurocholate uptake by MRP3. The initial rate of ATP-dependent [^{3}H]taurocholate uptake by MRP3 was measured at various taurocholate concentrations (1−32 μM) for 5 min at 37 °C. Data were plotted as V_0 versus [S] to confirm that the concentration range selected was appropriate to observe both zero-order and first-order rate kinetics. Kinetic parameters for taurocholate transport were determined from nonlinear regression analysis of the combined data and are provided in Results. Panel C: Effect of taurocholate on ATP-dependent [^{3}H]$E_2$17βG transport by MRP3. Membrane vesicles (5 μg of total proteins) were incubated at 37 °C in 25 μL of transport buffer containing 4 mM ATP, 10 mM $MgCl_2$ and [^{3}H]$E_2$17βG (400 nM, 100 nCi) for 1 min in the presence of various concentrations of taurocholate (1−1000 μM). IC_{50} values for the inhibition of [^{3}H]$E_2$17βG uptake by taurocholate were obtained from the best fit of the data to a sigmoidal curve. Details of IC_{50} values are provided in Results. The transport assays were performed as described. Values shown are the mean ± SD of three independent experiments. The transfectants tested were HEK_{pC7} (□, ■), HEK_{MRP3} (△, ▲). Closed symbols represent uptake in the presence of 4 mM ATP; open symbols represent uptake in the presence of 4 mM AMP.

detectable effect. However, mutations S1229A, S1231A, Y1232F, S1233A, and N1241A all reduced methotrexate transport activity. Similar to the results obtained with E_2-17βG as a substrate, substitution of Thr^{1237} with Ala resulted in a mutant protein that displayed an enhanced transport activity of the drug.

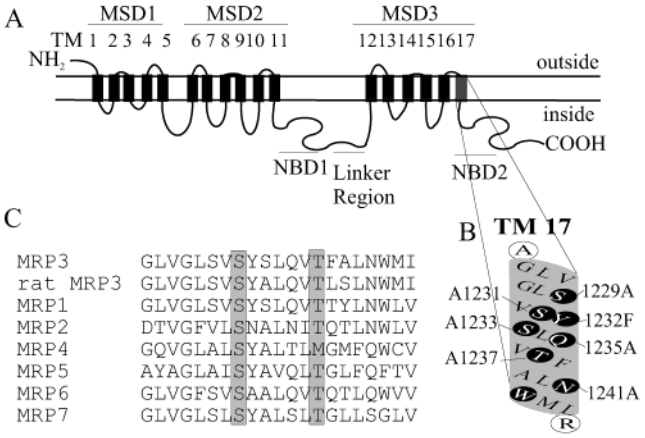

FIGURE 3: Topology of human MRP3. Panel A: Predicted topology of human MRP3 with 17 transmembrane (TM) helices. The putative TM17 is indicated by a lighter shading. Panel B: Expanded view of TM17. Residues with a side chain capable of hydrogen bonding are indicated by shaded circles. Panel C: Sequence alignment of the predicted TM17 of human and rat MRP3 and human MRP1, -2, -4, -5, -6, and -7. The alignment is obtained using Dnaman Multiple Sequence Fast Alignment II.

Having confirmed that human MRP3 transports taurocholate, we also determined the effects of TM17 mutations on transport of this substrate (Figure 6). Mutations S1229A, S1231A, and N1241A did not significantly influence transport activity. However, mutations Y1232F and S1233A both decreased taurocholate transport activity by approximately 30−50%. In contrast, mutations Q1235A and T1237A increased the ability of MRP3 to transport the bile salt approximately 1.5- and 3-fold, respectively. Thus, polar amino acid residues Ser^{1229}, Ser^{1231}, Gln^{1235}, and Asn^{1241} influenced the substrate specificity of MRP3, whereas residues Tyr^{1232}, Ser^{1233}, and Thr^{1237} affected the ability of MRP1 to transport all three substrates tested.

Kinetic Parameters of [^{3}H]Taurocholate and [^{3}H]$E_2$17βG Transport by Wild-Type MRP3 and Mutants MRP3^{Q1235A} and MRP3^{T1237A}. We have shown that mutation T1237A increased the ability of MRP3 to transport both $E_2$17βG and taurocholate. Like mutation T1237A, replacement of Gln^{1235} with Ala also increased taurocholate uptake. However, this mutation decreased $E_2$17βG transport. Thus, to determine the influences of the two mutations on $E_2$17βG and taurocholate transport more precisely, we compared K_m and V_{max} values for the wild-type protein with mutants MRP3^{Q1235A} and MRP3^{T1237A} (Figure 7). For wild-type and mutant MRP3, the K_m values for taurocholate transport were essentially identical (30.4 ± 9.3 μM for wild-type MRP3; 37.2 ± 3.4 and 32.8 ± 4.2 μM for MRP3^{Q1235A} and MRP3^{T1237A}, respectively) (Figure 7A, Table 1). In contrast, the V_{max} values for mutants MRP3^{Q1235A} and MRP3^{T1237A} [1417 ± 109 and 1669 ± 134 pmol mg^{-1} (5 min)$^{-1}$ for MRP3^{Q1235A} and MRP3^{T1237A}, respectively] were approximately 3−4-fold higher than that for the wild-type protein [464 ± 84 pmol mg^{-1} (5 min)$^{-1}$]. The results suggest that mutations Q1235A and T1237A affect a step in the transport process after initial binding of this substrate.

The effects of mutations Q1235A and T1237A on kinetic parameters of $E_2$17βG transport were also examined (Figure 7B, Table 1). Mutation Q1235A had no significant effect on the K_m values (29 and 32 μM for wild-type MRP3 and mutant MRP1^{Q1235A}, respectively) but decreased the V_{max}

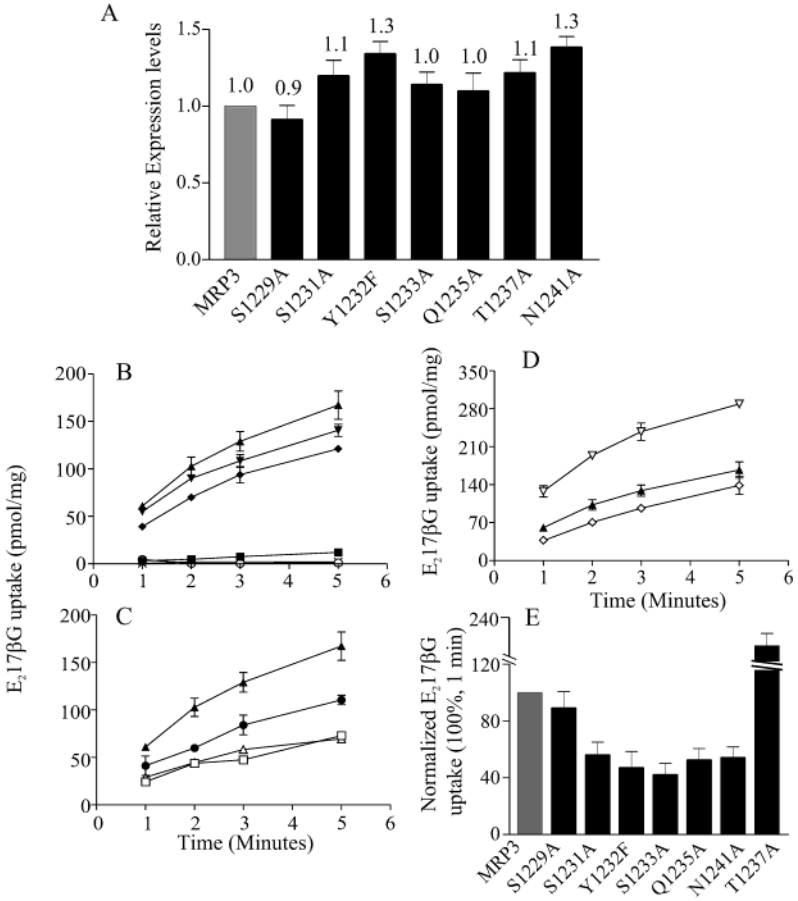

FIGURE 4: ATP-dependent [^{3}H]$E_2$17βG uptake by membrane vesicles prepared from HEK293 cells stably transfected with wild-type or mutant MRP3. Panel A: Relative protein expression levels of wild-type and mutant MRP3 proteins in stably transfected HEK293 cells. Expression levels were determined by immunoblotting and densitometry as described. The numbers above the bar refer to the levels of the mutant MRP3 proteins relative to wild-type MRP3 proteins in membrane vesicles prepared from the stably transfected HEK293 cells. Values shown are the mean ± SD of nine independent experiments. Panels B−D: ATP-dependent [^{3}H]$E_2$17βG uptake. Briefly, membrane vesicles were incubated at 37 °C with $E_2$17βG (400 nM, 100 nCi) in transport buffer for the time indicated, as described. Transfectants tested were HEK_{pC7} (■), HEK_{MRP3} (▲), $HEK_{MRP3S1229A}$ (▼), $HEK_{MRP3S1231A}$ (◆), $HEK_{MRP3Y1232F}$ (●), $HEK_{MRP3S1233A}$ (□), $HEK_{MRP3Q1235A}$ (△), $HEK_{MRP3T1237A}$ (▽), and $HEK_{MRP3N1241A}$ (◇). The uptake of $E_2$17βG by membrane vesicles prepared from control and wild-type MRP3-transfected HEK293 cells in transport buffer containing 4 mM AMP was also examined and shown in panel B [HEK_{pC7} (○) and HEK_{MRP3} (+)]. Panel E: Relative levels of [^{3}H]$E_2$17βG uptake at 1 min after subtracting uptake by membrane vesicles prepared from cells transfected with the control pCEBC7 vector and normalizing mutant MRP3 protein levels to wild-type MRP3 protein levels. Data shown in panels B−D have not been normalized to compensate for differences in expression levels. Values are the mean ± SD of three independent experiments.

value approximately 3-fold [V_{max} = 2204 and 728 pmol mg^{-1} min^{-1} for wild-type MRP3 and MRP1^{Q1235A}, respectively]. Thus, similar to the results obtained with taurocholate as a substrate, mutation Q1235A appeared not to influence the initial binding of the conjugated estrogen to the protein. Interestingly, converting Thr^{1237} to Ala decreased K_m values for $E_2$17βG transport by approximately 5-fold (K_m = 6 μM for MRP1^{T1237A}). The mutation also resulted in an approximately 2-fold reduction in V_{max} (1147 pmol mg^{-1} min^{-1}) value for $E_2$17βG transport (Table 1). Thus, in contrast to the results obtained with taurocholate, these findings demonstrated that the increase in $E_2$17βG transport observed with the T1237A mutation at subsaturating concentrations was attributable to increased affinity of the protein for this substrate, which is associated with a decrease in V_{max}.

Effect of Mutations on Resistance to VP-16 Conferred by MRP3. The effect of the mutant proteins on resistance to VP-16 was also examined (Table 2). As observed with the effects of the mutations on $E_2$17βG transport, substitution of Ser^{1229} with Ala did not influence the ability of MRP3 to confer VP-16 resistance. However, mutation of five hydrophilic amino acid residues (S1231A, Y1232F, S1233A, Q1235A, and N1241A) caused approximately a 2−3-fold reduction of resistance to VP-16. Interestingly, conversion of Thr^{1237} to Ala resulted in a mutant protein with enhanced resistance to VP-16 (3-fold). Thus, on the basis of the substrates tested in this study, mutations S1229A, S1231A, Q1235A, and N1241A affected substrate specificity of MRP3, whereas mutations Y1232F, S1233A, and T1237A influenced the overall activity of the protein.

Effect of Mutations T1237G, T1237S, and T1237L on VP-16 Resistance. Since replacement of Thr^{1237} with Ala resulted in a mutant protein with an enhanced capacity to confer VP-16 resistance, we also mutated this residue to Gly, Ser, and Leu. These mutations were stably expressed in HEK293 cells, and the expression levels of the mutant proteins in stably transfected HEK293 cells were similar to that of wild-type MRP3 (Figure 8A). Resistance to VP-16 conferred by these mutants was then determined by MTT assay. As shown in Table 2, mutation T1237G, like T1237A, significantly

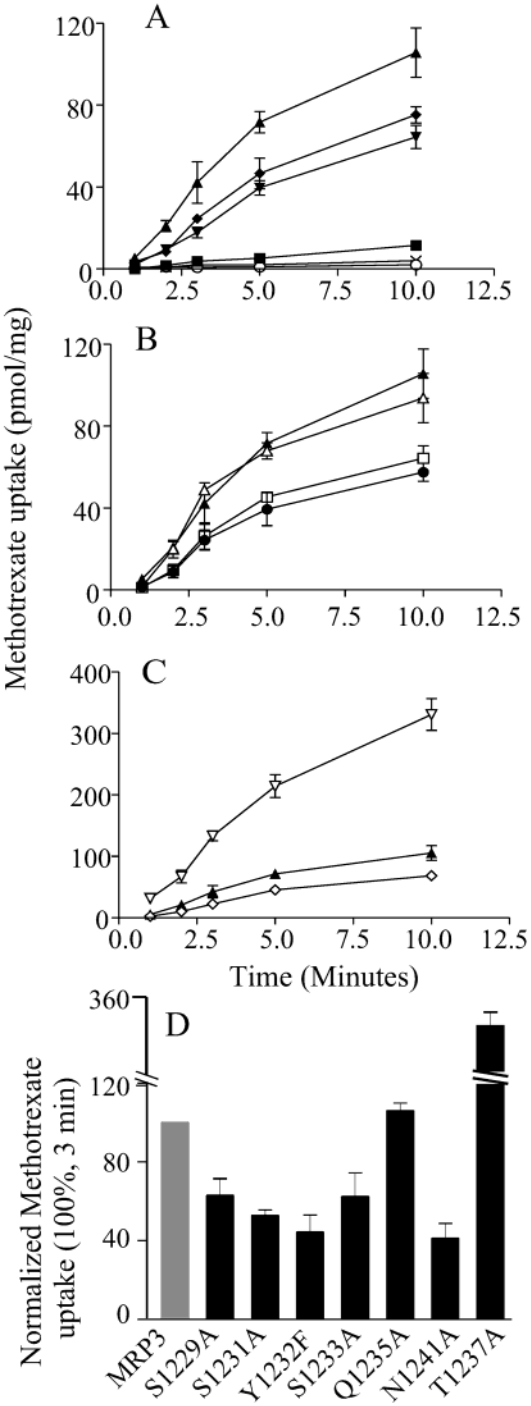

FIGURE 5: ATP-dependent [^{3}H]methotrexate uptake by membrane vesicles prepared from HEK293 cells stably transfected with wild-type or mutant MRP3. Membrane vesicles were incubated at 37 °C with 1 μM methotrexate in transport buffer as described in the legend to Figure 4. Transfectants tested were HEK_{pC7} (■), HEK_{MRP3} (▲), $HEK_{MRP3S1229A}$ (▼), $HEK_{MRP3S1231A}$ (◆), $HEK_{MRP3Y1232F}$ (●), $HEK_{MRP3S1233A}$ (□), $HEK_{MRP3Q1235A}$ (△), $HEK_{MRP3T1237A}$ (▽), and $HEK_{MRP3N1241A}$ (◇). The uptake of methotrexate by membrane vesicles prepared from control and wild-type MRP3-transfected HEK293 cells in transport buffer containing 4 mM AMP was also examined and shown in panel A [HEK_{pC7} (○) and HEK_{MRP3} (+)]. Panel D: Relative levels of [^{3}H]methotrexate uptake at 3 min after subtracting uptake by membrane vesicles prepared from cells transfected with the control pCEBC7 vector and normalizing mutant MRP3 protein levels to wild-type MRP3 protein levels. Data shown in panels A−C have not been normalized to compensate for differences in expression levels. Values are the mean ± SD of three independent experiments.

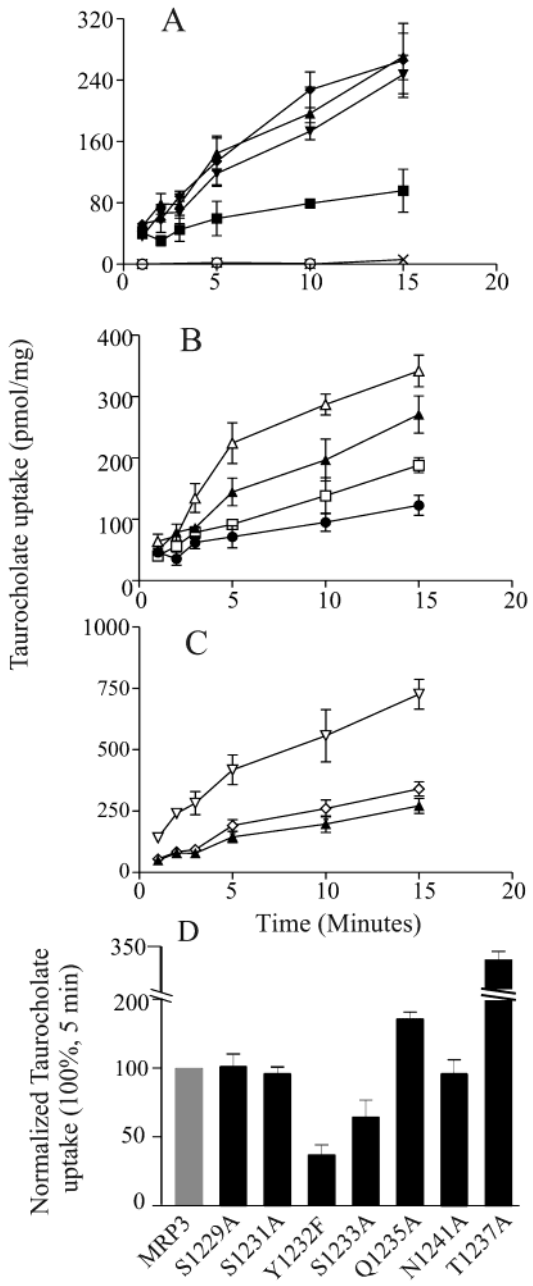

FIGURE 6: ATP-dependent [^{3}H]taurocholate uptake by membrane vesicles prepared from HEK293 cells stably transfected with wild-type or mutant MRP3. Membrane vesicles were incubated at 37 °C with 4 μM taurocholate in transport buffer as described in the legend to Figure 4. Transfectants tested were HEK_{pC7} (■), HEK_{MRP3} (▲), $HEK_{MRP3S1229A}$ (▼), $HEK_{MRP3S1231A}$ (◆), $HEK_{MRP3Y1232F}$ (●), $HEK_{MRP3S1233A}$ (□), $HEK_{MRP3Q1235A}$ (△), $HEK_{MRP3T1237A}$ (▽), and $HEK_{MRP3N1241A}$ (◇). The uptake of taurocholate by membrane vesicles prepared from control and wild-type MRP3-transfected HEK293 cells in transport buffer containing 4 mM AMP was also examined and shown in panel A [HEK_{pC7} (○) and HEK_{MRP3} (+)]. Panel D: Relative levels of [^{3}H]taurocholate uptake at 5 min after subtracting uptake by membrane vesicles prepared from cells transfected with the control pCEBC7 vector and normalizing mutant MRP3 protein levels to wild-type MRP3 protein levels. Data shown in panels A−C have not been normalized to compensate for differences in expression levels. Values are the mean ± SD of three independent experiments.

increased the ability of MRP3 to confer VP-16 resistance. Substitution of Thr^{1237} with Leu only moderately enhanced resistance to VP-16. However, conversion of Thr^{1237} to a

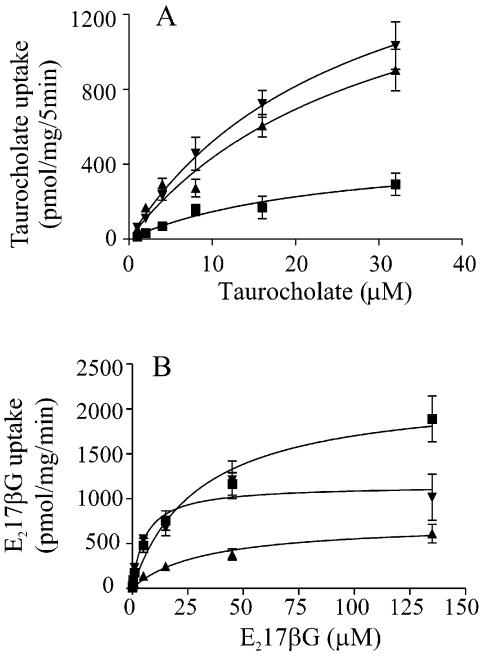

FIGURE 7: Kinetics of ATP-dependent [^{3}H]taurocholate (panel A) and [^{3}H]$E_2$17βG (panel B) uptake by wild-type and mutant proteins. The initial rate of ATP-dependent [^{3}H]taurocholate uptake (panel A) by membrane vesicles prepared from HEK293 cells transfected with wild-type or mutant proteins was measured at various taurocholate concentrations (1−32 μM) for 5 min at 37 °C as described. [^{3}H]$E_2$17βG uptake (panel B) was determined as described for [^{3}H]taurocholate except that the reactions were carried out with various concentrations of $E_2$17βG (0.1−135 μM) for 1 min. Values are the mean ± SD of triplicate determinations in a single experiment. Similar results were obtained from one more experiment. Data were plotted as V_0 versus [S] to confirm that the concentration range selected was appropriate to observe both zero-order and first-order rate kinetics. The transfectants tested were HEK_{MRP3} (■), $HEK_{MRP3Q1235A}$ (▲), and $HEK_{MRP3T1237A}$ (▼). Kinetic parameters for $E_2$17βG and taurocholate transport were determined from nonlinear regression analysis of the combined data and shown in Table 1.

conserved residue, Ser, decreased resistance to the chemotherapeutic by approximately 50%. These findings suggest that the size together with the hydrophobicity of the side chain of the residue at position 1237 plays an important role in determining the ability of MRP3 to confer VP-16 resistance.

Effects of Mutations T1237G, T1237S, and T1237L on the Transport Profile of MRP3. In addition to the effect on VP-16 resistance, substitution of Thr^{1237} with Ala increased the capacity of MRP3 to transport methotrexate, $E_2$17βG, and taurocholate. Thus, the effects of the mutations T1237G, T1237S, and T1237L on the ability of MRP3 to transport these three substrates were also examined by in vitro transport assays (Figure 8B−D). Replacement of Thr^{1237} with Gly, like mutation T1237A, dramatically increased the ability of MRP3 to transport methotrexate (Figure 8B), $E_2$17βG (Figure 8C), and taurocholate (Figure 8D). Converting Thr^{1237} to a conserved residue, Ser, had no significant effect on the transport of $E_2$17βG (Figure 8C) but dramatically reduced methotrexate transport activity (Figure 8B) while increasing taurocholate transport activity by approximately 50% (Figure 8D). Substitution of Thr^{1237} with a hydrophobic residue, Leu, moderately increased the transport activity of all three substrates tested (Figure 8B−D). These results further demonstrate that the size and hydrophobicity of the side chain of the residue at position 1237 are important for the function of MRP3.

DISCUSSION

Prior to examining the effects of various mutations on the substrate specificity of MRP3, we characterized the functional properties of the wild-type protein in stable HEK293 transfectants. Overexpression of MRP3 resulted in an increase in resistance to VP-16 quantitatively similar to that observed previously in HEK293 MRP1 transfectants (*13*). Using MRP1/MRP3 hybrid proteins as standards for immunoblotting, we were able to confirm that the level of expression of the two proteins was comparable. Thus MRP1 and MRP3 confer resistance to VP-16 with similar efficiency. Zeng et al. (*34*) reported that MRP3 also conferred a low level of resistance to vincristine. However, despite the relatively high level of VP-16 resistance obtained with our MRP3 transfectants when compared with other published reports (*34*, *37*), we did not detect resistance to other commonly used chemotherapeutic agents such as vincristine, doxorubicin, and cisplatin. This resistance profile is consistent with that obtained when MRP3 was expressed in Madin-Darby canine kidney II cells and in fibroblasts derived from mouse kidney (*35*, *37*). We also confirmed that MRP3 actively transports methotrexate and $E_2$17βG (K_m = 29.7 ± 6.2 μM), consistent with previous estimates (*35*, *38*).

Human MRP3 expressed in insect Sf21 cells or stably transfected HEK293 cells, unlike the rat orthologue, has been reported to be incapable of transporting taurocholate (*38*, *46*). However, we found previously, using short-term transfectants of HEK293 cells, that taurocholate transport by the human protein was readily detectable (*48*). The more extensive analyses reported here using vesicles prepared from the HEK293 stable transfectants indicate that human MRP3 transports taurocholate with an apparent affinity only approximately 2-fold lower (K_m for 30.4 μM) than that reported for the rat orthologue (K_m for 15.9 μM) (*45*). These values are similar to those reported recently using membrane vesicles isolated from insect cells expressing human MRP3 (*48*).

MRP1 and MRP3 are structurally the most similar members of the MRP family. However, although they share several common substrates, such as $E_2$17βG, methotrexate, and VP-16, their overall substrate specificity profiles differ substantially. Previously, we demonstrated that amino acids with hydrogen-bonding side chains that are clustered in the predicted inner-leaflet region of TM17 of MRP1 are important determinants of substrate specificity, including the ability to transport the common MRP1/MRP3 substrates $E_2$17βG and VP-16 (*59*) (Figure 9B). TM17 is strikingly conserved between MRP1 and MRP3 and is exceptionally rich in polar amino acids (Figure 9). Consequently, we examined to what extent the functions of comparable polar residues in this helix are conserved between the two proteins with respect to determining either substrate specificity or overall transport activity.

Crystallographic studies of independently evolved multidrug binding proteins, such as QacR and PXR, have revealed that polar residues are crucial for interaction of the proteins with their substrates (*63*, *64*). In the QacR−rhodamine 6G

Table 1: Kinetic Parameters of Taurocholate and $E_2 17\beta G$ Uptake by Vesicles from HEK Cells Transfected with Vectors Encoding Wild-Type and Mutant Proteins[a]

	K_m (μM)		V_{max}		normalized V_{max}		V_{max}/K_m	
transfectant	TC	$E_2 17\beta G$	TC [pmol mg^{-1} (5 min)$^{-1}$]	$E_2 17\beta G$ [pmol mg^{-1} (5 min)$^{-1}$]	TC	$E_2 17\beta G$	TC	$E_2 17\beta G$
HEK_{MRP3}	30	29	464	2204	464	2204	15	76
$HEK_{MRP3Q1235A}$	37	32	1417	728	1417	728	38	23
$HEK_{MRP3T1237A}$	33	6	1669	1147	1517	1043	46	174

[a] The kinetic parameters of taurocholate (TC) and $E_2 17\beta G$ uptake were determined as described in the legend to Figure 7. The normalized V_{max} values were obtained by adjusting determined V_{max} values to compensate for differences in the relative levels of the wild-type and mutant proteins.

Table 2: Resistance to VP-16 Conferred by Wild-Type and Mutant MRP3[a]

	drug (VP-16)		
transfectant	IC_{50} (μM)	RRF	$RRF^{mutantMRP3}/RRF^{MRP3}$ (%)
HEK_{pC7}	0.171 ± 0.033	1	
HEK_{MRP3}	0.937 ± 0.152	5.4 ± 0.9 (5.4)	100
HEK_{S1229A}	0.809 ± 0.119	4.7 ± 0.7 (5.2)	96
HEK_{S1231A}	0.456 ± 0.089	2.7 ± 0.5 (2.5)	46
HEK_{Y1232F}	0.383 ± 0.087	2.2 ± 0.5 (1.7)	31
HEK_{S1233A}	0.579 ± 0.090	3.4 ± 0.5 (3.4)	62
HEK_{Q1235A}	0.551 ± 0.075	3.2 ± 0.4 (3.2)	59
HEK_{T1237A}	2.915 ± 0.591	17.1 ± 3.4 (17.1)	317
HEK_{N1241A}	0.577 ± 0.125	3.4 ± 0.7 (2.6)	48
HEK_{T1237G}	2.230 ± 0.297	13.0 ± 1.8 (16.3)	302
HEK_{T1237L}	1.433 ± 0.152	8.4 ± 0.9 (9.4)	174
HEK_{T1237S}	0.589 ± 0.120	3.4 ± 0.7 (3.1)	57

[a] The resistance of HEK293 cells transfected with expression vectors encoding wild-type and mutant MRP3 relative to that of cells transfected with empty vector was determined using a tetrazolium salt-based microtiter plate assay. Data were analyzed as described. The relative resistance factor (RRF) was obtained by dividing the IC_{50} values for wild-type/mutant MRP3-transfected cells by the IC_{50} value for control transfectants. The values shown represent the mean ± SD of IC_{50}'s determined from three to six independent experiments. Resistance factors normalized for differences in the levels of mutant proteins expressed in the transfectant populations used are shown in parentheses.

complex, hydrophilic residues Gln^{64}, Thr^{89}, and Gln^{96}, located in the ligand binding cavity, provide versatility for contacting polar moieties of the drug (*63*). It has also been demonstrated that polar residues Asn, Gln, Asp, and Glu, located in transmembrane α-helices of multispanning TM proteins, play an important role in the stabilization of helix−helix interactions through participating in interhelical hydrogen bonds (*65*−*67*). In addition, the hydroxyl groups of Ser and Thr in transmembrane α-helices have been shown to participate in shared hydrogen bonds to carbonyl oxygens in the preceding turn of the helix, stabilizing the transmembrane domains (*68*, *69*). Thus mutations that eliminate side chain hydrogen-bonding potential may influence the function of the protein, not only by directly altering interactions with substrate but also by decreasing H-bonding between and within TM helices.

Mutations that selectively affect certain compounds and not others appear more likely candidates for direct interaction with specific substrates, while those with pleiotropic effects on activity may play a more general role in defining the conformation and stability of the protein in the vicinity of a substrate binding pocket. We initially assessed whether residues that affected overall activity were conserved between the two proteins. In MRP3, elimination of the hydrogen-bonding capability of Tyr^{1232} and Ser^{1233} negatively affected all functions, while mutation of Thr^{1237} to Ala had a positive effect. In contrast to the pleiotropic effects of these mutations, the comparable residues, Tyr^{1236} and Thr^{1241}, in MRP1 selectively and negatively affected only resistance to vincristine, while Ser^{1237} had no discernible effect on either substrate specificity or overall activity. Similarly, mutation of Ser^{1233} and Ser^{1235} of MRP1 also had no effect on any function tested. In contrast, mutation of Ser^{1229} in MRP3 decreased methotrexate transport, and mutation of Ser^{1231} decreased both methotrexate and E217βG transport, as well as resistance to VP-16. Thus, despite the very high level of sequence identity, there appears to be little functional conservation between the two proteins with respect to specific residues predicted to be in the outer-leaflet region of TM17.

In MRP1, we found that mutation of polar residues predicted to be proximal to the membrane/cytoplasm interface affected either the overall activity or substrate specificity of the protein (*59*) (Figure 9B). However, Tyr^{1243} or Thr^{1242}, both of which appear to be important for the overall activity of MRP1, are not conserved in MRP3. The only conserved residue identified in the inner-leaflet region of TM17 that appears to share some functional characteristics is Asn^{1241} in MRP3 and Asn^{1245} in MRP1. Mutation of these residues to Ala decreased the ability of both proteins to confer resistance to VP-16 and to transport $E_2 17\beta G$.

It is particularly apparent in the case of MRP3 that all of the polar residues in TM17 which affect substrate specificity or overall activity cannot be located on the same side of a typical amphipathic α-helix (Figure 9A). Thus it appears extremely unlikely that all polar residues can be exposed simultaneously to an aqueous pore that might serve as a pathway through the membrane for some hydrophilic substrates, as recently proposed for the bacterial transporter, Lmra (*70*). However, the three polar amino acids in TM17 of MRP3 that affect overall activity are predicted to be on one side of the helix (Ser^{1232}, Ser^{1233}, and Thr^{1237}), while those that have a more selective effect on substrate specificity, with the exception of Ser^{1229}, are on the opposing side (Figure 9A). Based on known structures of ABC proteins, it is difficult to predict whether those residues affecting specificity are exposed while those that affect overall activity are involved in inter- or intrahelical interactions. Cross-linking studies in P-gp have shown that TM12 of P-gp, which is comparable to TM17 of MRP3, due to the five additional NH_2-proximal transmembrane helices, and may form part of a potential drug binding pocket in P-gp, is close to TM6, which is comparable to TM11 of MRP3 (*71*). Crystal structures of the half-ABC transporter MsbA show that TM6 of MsbA is close to TM5 (*75*), which corresponds to TM16 of MRP3. Studies of MRP1 with photoactivatable ligands

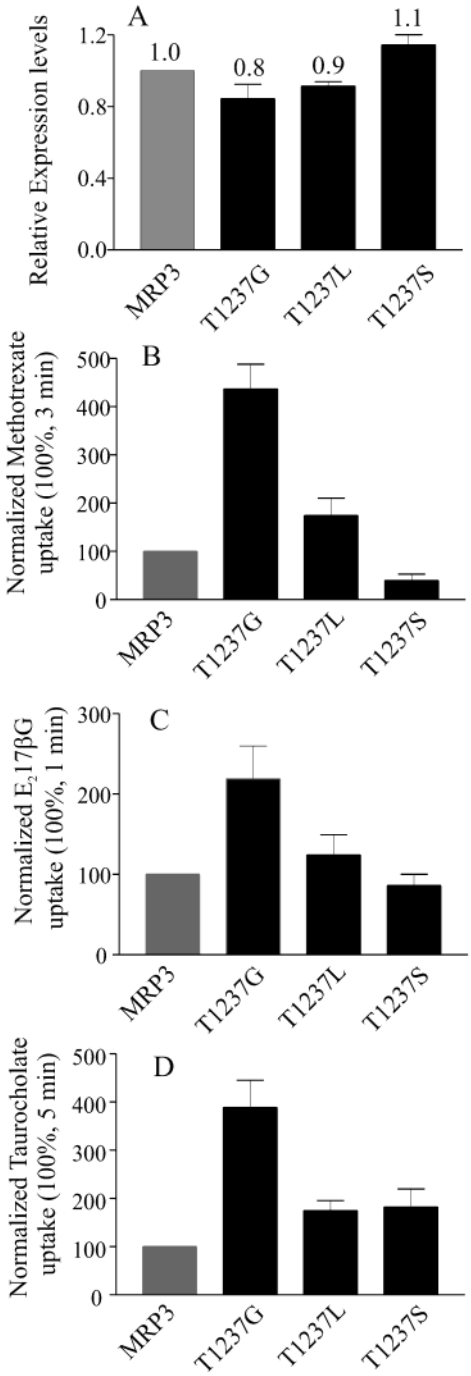

FIGURE 8: Effect of mutations T1237S, T1237L, and T1237G on ATP-dependent [^{3}H]methotrexate (panel B), [^{3}H]E$_2$17βG (panel C), and [^{3}H]taurocholate (panel D) uptake by wild-type MRP3. Relative protein expression levels of wild-type and mutant MRP3 proteins in stably transfected HEK293 cells were determined (panel A) as described in the legend to Figure 4. The numbers above the bar refer to the levels of the mutant MRP3 proteins relative to wild-type MRP3 proteins in membrane vesicles prepared from the stably transfected HEK293 cells. Values shown are the mean ± SD of nine independent experiments. Panels B−D: Relative levels of [^{3}H]-methotrexate (panel B, at 3 min), [^{3}H]E$_2$17βG (panel C, at 1 min), and [^{3}H]taurocholate (panel D, at 5 min) uptake after subtracting uptake by membrane vesicles prepared from cells transfected with the control pCEBC7 vector and normalizing mutant MRP3 protein levels to wild-type MRP3 protein levels. Values are the mean ± SD of three independent experiments.

have implicated TMs 10 and 11 and TMs 16 and 17 in substrate binding (*72*). Consequently, the polar residues in

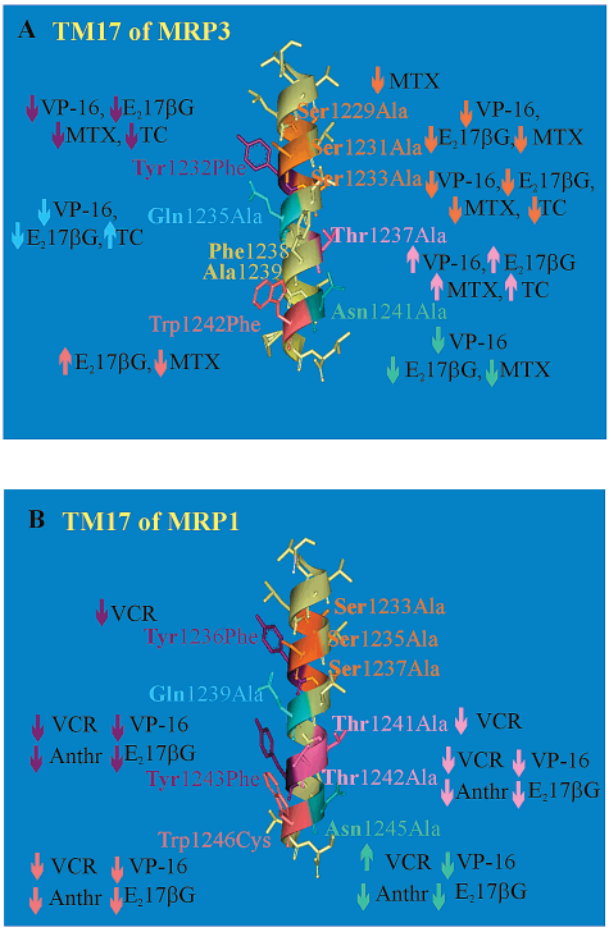

FIGURE 9: Models of TM17 of MRP3 and MRP1 and a helical wheel projection of TM17 of MRP3. Panels A and B: The figures illustrate the predicted three-dimensional structures for TM17 of MRP3 and MRP1 obtained using Sybyl and WebLab ViewerPro. The qualitative effects of mutating each of the residues with respect to drug resistance and transport activities are also shown.

TM17 of MRP3 might participate in inter- or intrahelical hydrogen bonds that are important for the overall topography of a substrate binding pocket. The only available crystal structures of the membrane-spanning domains of ABC transporters are limited to prokaryotic members of the superfamily, and their sequence similarity to MRP1 is at the lower limit of modeling algorithms. As a result, it is difficult to predict with any reliability which of the polar residues in TM17 might project into a hydrophilic pore. Furthermore, it is known that ATP binding or hydrolysis by proteins such as P-gp and MRP1 induces a conformational change that markedly decreases the affinity for substrate (*73*). It is commonly assumed that this conformational change influences the spatial organization of TM helices. If this involves rotation of helices such as TM17, polar residues exposed in an aqueous pore may change during transport of substrate. Consequently, some residues that affect specificity may influence interactions with substrate after the initial binding step, during or after the transition from a high- to low-affinity conformation. Consistent with this possibility, mutation Q1235A increased and decreased the V_{max} for transport of taurocholate and E$_2$17βG, respectively, without affecting the K_m for either substrate.

Although the majority of mutations that eliminated hydrogen-bonding potential had a negative effect on the activity

of the protein, there were two exceptions. Mutation Q1235A caused a decrease in VP-16 resistance and $E_2$17βG transport, consistent with the involvement of hydrogen bonding in the interaction with these substrates, but the mutation increased taurocholate transport. Previous studies in MRP1 and P-gp suggest that the size of the amino acid side chain also affects substrate specificity, with small side chains favoring interaction with larger substrates (*59*, *74*). Consistent with this suggestion, among the three hydrophilic substrates tested in this study ($E_2$17βG, methotrexate, and taurocholate), taurocholate is the largest. In addition, conversion of polar residue Thr^{1237} to either Ala or Gly markedly increased the ability to confer VP-16 resistance and to transport $E_2$17βG, taurocholate, and methotrexate, while mutation to a bulkier and more hydrophobic Leu residue resulted in only a moderate increase in transport of all three substrates. The effect of replacement of Thr^{1237} with Ser was more complex. This mutation dramatically decreased methotrexate transport and VP-16 resistance but had no significant effect on the transport of $E_2$17βG, while moderately increasing taurocholate transport. These results demonstrate that the size together with the hydrophobicity of the residue side chain at position 1237 is crucial for determining the substrate specificity of MRP3. Interestingly, although mutation T1237A increased the ability of MRP3 to transport both taurocholate and $E_2$17βG, the mutation resulted in a major increase in V_{max} for taurocholate uptake, without significantly affecting K_m values. In contrast, this mutation decreased both K_m and V_{max} values for $E_2$17βG transport, suggesting that the mutation increased the affinity of MRP3 for the conjugated estrogen. One possible explanation for these observations is that Thr^{1237} may be involved in the binding of taurocholate to a low-affinity site and that elimination of its hydrogen-bonding capacity may facilitate substrate release. If so, the fact that the T1237A mutations increase the affinity of the protein for $E_2$17βG suggests that a single amino acid may contribute both to the high-affinity binding of one substrate and the low-affinity binding of another.

In summary, we found that polar residues in the putative TM17 of MRP3 are involved in overall function and/or substrate specificity of MRP3. Some of these residues are highly conserved among different MRPs (Figure 3). However, as shown in Figure 9, conserved amino acid residues such as Ser^{1231}, Tyr^{1232}, Thr^{1237}, and Trp^{1242} in MRP3 and the comparable residues Ser^{1235}, Tyr^{1236}, Thr^{1241}, and Trp^{1246} in MRP1 do not make similar contributions to their ability to transport common substrates. Overall, these studies demonstrate that the conservation of overlapping substrate specificities by these two transporters is evolutionarily complex and cannot be predicted from the conservation of primary structure, even in highly conserved regions that are clearly critical for substrate recognition and transport.

ACKNOWLEDGMENT

The authors thank Jimmy Zheng for assistance with preparation of Figure 9.

REFERENCES

1. Deeley, R. G., and Cole, S. P. C. (1997) *Semin. Cancer Biol. 8*, 193−204.
2. Cole, S. P. C., Bhardwaj, G., Gerlach, J. H., Mackie, J. E., Grant, C. E., Almquist, K. C., Stewart, A. J., Kurz, E. U., Duncan, A. M., and Deeley, R. G. (1992) *Science 258*, 1650−1654.
3. Borst, P., and Elferink, R. O. (2002) *Annu. Rev. Biochem. 71*, 537−592.
4. Borst, P., Evers, R., Kool, M., and Wijnholds, J. (2000) *J. Natl. Cancer Inst. 92*, 1295−1302.
5. Leslie, E. M., Deeley, R. G., and Cole, S. P. C. (2001) *Toxicology 167*, 3−23.
6. Hipfner, D. R., Deeley, R. G., and Cole, S. P. C. (1999) *Biochim. Biophys. Acta 1461*, 359−376.
7. Gottesman, M. M., Fojo, T., and Bates, S. E. (2002) *Nat. Rev. Cancer 2*, 48−58.
8. Bates, S. E., Robey, R., Miyake, K., Rao, K., Ross, D. D., and Litman, T. (2001) *J. Bioenerg. Biomembr. 33*, 503−511.
9. Litman, T., Brangi, M., Hudson, E., Fetsch, P., Abati, A., Ross, D. D., Miyake, K., Resau, J. H., and Bates, S. E. (2001) *J. Cell Sci. 113*, 2011−2021.
10. Doyle, L. A., Yang, W., Abruzzo, L. V., Krogmann, T., Gao, Y., Rishi, A. K., and Ross, D. D. (1998) *Proc. Natl. Acad. Sci. U.S.A. 95*, 15665−15670.
11. Cole, S. P. C., Sparks, K. E., Fraser, K., Loe, D. W., Grant, C. E., Wilson, G. M., and Deeley, R. G. (1994) *Cancer Res. 54*, 5902−5910.
12. Zaman, G. J., Flens, M. J., van Leusden, M. R., de Haas, M., Mulder, H. S., Lankelma, J., Pinedo, H. M., Scheper, R. J., Baas, F., and Broxterman, H. J. (1994) *Proc. Natl. Acad. Sci. U.S.A. 91*, 8822−8826.
13. Stride, B. D., Grant, C. E., Loe, D. W., Hipfner, D. R., Cole, S. P. C., and Deeley, R. G. (1997) *Mol. Pharmacol. 52*, 344−353.
14. Breuninger, L. M., Paul, S., Gaughan, K., Miki, T., Chan, A., Aaronson, S. A., and Kruh, G. D. (1995) *Cancer Res. 55*, 5342−5347.
15. Loe, D. W., Almquist, K. C., Deeley, R. G., and Cole, S. P. C. (1996) *J. Biol. Chem. 271*, 9675−9682.
16. Loe, D. W., Almquist, K. C., Cole, S. P. C., and Deeley, R. G. (1996) *J. Biol. Chem. 271*, 9683−9689.
17. Jedlitschky, G., Leier, I., Buchholz, U., Barnouin, K., Kurz, G., and Keppler, D. (1996) *Cancer Res. 56*, 988−994.
18. Qian, Y. M., Song, W. C., Cui, H., Cole, S. P. C., and Deeley, R. G. (2001) *J. Biol. Chem. 276*, 6404−6411.
19. Leslie, E. M., Ito, K., Upadhyaya, P., Hecht, S. S., Deeley, R. G., and Cole, S. P. C. (2001) *J. Biol. Chem. 276*, 27846−27854.
20. Wijnholds, J., Mol, C. A., van Deemter, L., de Haas, M., Scheffer, G. L., Baas, F., Beijnen, J. H., Scheper, R. J., Hatse, S., De Clercq, E., Balzarini, J., and Borst, P. (2000) *Proc. Natl. Acad. Sci. U.S.A. 97*, 7476−7481.
21. Schuetz, J. D., Connelly, M. C., Sun, D., Paibir, S. G., Flynn, P. M., Srinivas, R. V., Kumar, A., and Fridland, A. (1999) *Nat. Med. 5*, 1048−1051.
22. Paulusma, C. C., Bosma, P. J., Zaman, G. J., Bakker, C. T., Otter, M., Scheffer, G. L., Scheper, R. J., Borst, P., and R. P. (1996) *Science 271*, 1126−1128.
23. Taniguchi, K., Wada, M., Kohno, K., Nakamura, T., Kawabe, T., Kawakami, M., Kagotani, K., Okumura, K., Akiyama, S., and Kuwano, M. (1996) *Cancer Res. 56*, 4124−4129.
24. Kiuchi, Y., Suzuki, H., Hirohashi, T., Tyson, C. A., and Sugiyama, Y. (1998) *FEBS Lett. 433*, 149−152.
25. Hopper, E., Belinsky, M. G., Zeng, H., Tosolini, A., Testa, J. R., and Kruh, G. D. (2001) *Cancer Lett. 162*, 181−191.
26. Yabuuchi, H., Shimizu, H., Takayanagi, S., and Ishikawa, T. (2001) *Biochem. Biophys. Res. Commun. 288*, 933−939.
27. Bera, T. K., Lee, S., Salvatore, G., Lee, B., and Pastan, I. (2001) *Mol. Med. 7*, 509−516.
28. Tammur, J., Prades, C., Arnould, I., Rzhetsky, A., Hutchinson, A., Adachi, M., Schuetz, J. D., Swoboda, K. J., Ptacek, L. J., Rosier, M., Dean, M., and Allikmets, R. (2001) *Gene 273*, 89−96.
29. Kao, H., Huang, J., and Chang, M. (2002) *Gene 286*, 299−306.
30. Hipfner, D. R., Almquist, K. C., Leslie, E. M., Gerlach, J. H., Grant, C. E., Deeley, R. G., and Cole, S. P. C. (1997) *J. Biol. Chem. 272*, 23623−23630.
31. Bakos, E., Hegedus, T., Hollo, Z., Welker, E., Tusnady, G. E., Zaman, G. J., Flens, M. J., Varadi, A., and Sarkadi, B. (1996) *J. Biol. Chem. 271*, 12322−12326.
32. Kast, C., and Gros, P. (1998) *Biochemistry 37*, 2305−2313.
33. Kast, C., and Gros, P. (1997) *J. Biol. Chem. 272*, 26479−26487.
34. Zeng, H., Bain, L. J., Belinsky, M. G., and Kruh, G. D. (1999) *Cancer Res. 59*, 5964−5967.
35. Zelcer, N., Saeki, T., Reid, G., Beijnen, J. H., and Borst, P. (2001) *J. Biol. Chem. 276*, 46400−46407.

36. Zeng, H., Chen, Z. S., Belinsky, M. G., Rea, P. A., and Kruh, G. D. (2001) *Cancer Res. 61*, 7225−7232.
37. Kool, M., van der, L. M., de Haas, M., Scheffer, G. L., de Vree, J. M., Smith, A. J., Jansen, G., Peters, G. J., Ponne, N., Scheper, R. J., Elferink, R. P., Baas, F., and Borst, P. (1999) *Proc. Natl. Acad. Sci. U.S.A. 96*, 6914−6919.
38. Zeng, H., Liu, G., Rea, P. A., and Kruh, G. D. (2000) *Cancer Res. 60*, 4779−4784.
39. Decleves, X., Fajac, A., Lehmann-Che, J., Tardy, M., Mercier, C., Hurbain, I., Laplanche, J. L., Bernaudin, J. F., and Scherrmann, J. M. (2002) *Int. J. Cancer 98*, 173−180.
40. Kawai, H., Kiura, K., Tabata, M., Yoshino, T., Takata, I., Hiraki, A., Chikamori, K., Ueoka, H., Tanimoto, M., and Harada, M. (2002) *Lung Cancer 35*, 305−314.
41. Nies, A. T., Konig, J., Pfannschmidt, M., Klar, E., Hofmann, W. J., and Keppler, D. (2001) *Int. J. Cancer 94*, 492−499.
42. Rost, D., Konig, J., Weiss, G., Klar, E., Stremmel, W., and Keppler, D. (2001) *Gastroenterology 121*, 1203−1208.
43. Haga, S., Hinoshita, E., Ikezaki, K., Fukui, M., Scheffer, G. L., Uchiumi, T., and Kuwano, M. (2001) *Jpn. J. Cancer Res. 92*, 211−219.
44. Hirohashi, T., Suzuki, H., and Sugiyama, Y. (1999) *J. Biol. Chem. 274*, 15181−15185.
45. Hirohashi, T., Suzuki, H., Takikawa, H., and Sugiyama, Y. (2000) *J. Biol. Chem. 275*, 2905−2910.
46. Akita, H., Suzuki, H., Hirohashi, T., Takikawa, H., and Sugiyama, Y. (2002) *Pharm. Res. 19*, 34−41.
47. Zelcer, N., Saeki, T., Bot, I., Kuil, A., and Borst, P. (2003) *Biochem. J. 369*, 23−30.
48. Oleschuk, C. J., Deeley, R. G., and Cole, S. P. C. (2003) *Am. J. Physiol. Gastrointest. Liver Physiol. 284*, G280−G289.
49. Scheffer, G. L., Kool, M., de Haas, M., de Vree, J. M., Pijnenborg, A. C., Bosman, D. K., Elferink, R. P., van, d., V, Borst, P., and Scheper, R. J. (2002) *Lab. Invest. 82*, 193−201.
50. Cherrington, N. J., Hartley, D. P., Li, N., Johnson, D. R., and Klaassen, C. D. (2002) *J. Pharmacol. Exp. Ther. 300*, 97−104.
51. Rost, D., Mahner, S., Sugiyama, Y., and Stremmel, W. (2002) *Am. J. Physiol. Gastrointest. Liver Physiol. 282*, G720−G726.
52. Soroka, C. J., Lee, J. M., Azzaroli, F., and Boyer, J. L. (2001) *Hepatology 33*, 783−791
53. Scheffer, G. L., Kool, M., de Haas, M., de Vree, J. M., Pijnenborg, A. C., Bosman, D. K., Elferink, R. P., van, d., V, Borst, P., and Scheper, R. J. (2002) *Lab. Invest. 82*, 193−201.
54. Inokuchi, A., Hinoshita, E., Iwamoto, Y., Kohno, K., Kuwano, M., and Uchiumi, T. (2001) *J. Biol. Chem. 276*, 46822−46829.
55. Donner, M. G., and Keppler, D. (2001) *Hepatology 34*, 351−359.
56. Shoda, J., Kano, M., Oda, K., Kamiya, J., Nimura, Y., Suzuki, H., Sugiyama, Y., Miyazaki, H., Todoroki, T., Stengelin, S., Kramer, W., Matsuzaki, Y., and Tanaka, N. (2001) *Am. J. Gastroenterol. 96*, 3368−3378.
57. Akita, H., Suzuki, H., and Sugiyama, Y. (2001) *Pharm. Res. 18*, 1119−1125.
58. Ito, K., Suzuki, H., and Sugiyama, Y. (2001) *Am. J. Physiol. Gastrointest. Liver Physiol. 281*, G1034−G1043.
59. Zhang, D. W., Cole, S. P. C., and Deeley, R. G. (2002) *J. Biol. Chem. 277*, 20934−20941.
60. Zhang, D. W., Cole, S. P. C., and Deeley, R. G. (2001) *J. Biol. Chem. 276*, 34966−34974.
61. Ito, K., Olsen, S. L., Qiu, W., Deeley, R. G., and Cole, S. P. C. (2001) *J. Biol. Chem. 276*, 15616−15624.
62. Zhang, D. W., Cole, S. P. C., and Deeley, R. G. (2001) *J. Biol. Chem. 276*, 13231−13239.
63. Schumacher, M. A., Miller, M. C., Grkovic, S., Brown, M. H., Skurray, R. A., and Brennan, R. G. (2001) *Science 294*, 2158−2163.
64. Watkins, R. E., Wisely, G. B., Moore, L. B., Collins, J. L., Lambert, M. H., Williams, S. P., Willson, T. M., Kliewer, S. A., and Redinbo, M. R. (2001) *Science 292*, 2329−2333.
65. Partridge, A. W., Melnyk, R. A., and Deber, C. M. (2002) *Biochemistry 41*, 3647−3653.
66. Zhou, F. X., Merianos, H. J., Brunger, A. T., and Engelman, D. M. (2001) *Proc. Natl. Acad. Sci. U.S.A. 98*, 2250−2255.
67. Zhou, F. X., Cocco, M. J., Russ, W. P., Brunger, A. T., and Engelman, D. M. (2000) *Nat. Struct. Biol. 7*, 154−160.
68. Popot, J. L., and Engelman, D. M. (2000) *Annu. Rev. Biochem. 69*, 881−922.
69. Gray, T. M., and Matthews, B. W. (1984) *J. Mol. Biol. 175*, 75−81.
70. Poelarends, G. J., and Konings, W. N. (2002) *J. Biol. Chem. 277*, 42891−42898.
71. Loo, T. W., and Clarke, D. M. (1997) *J. Biol. Chem. 272*, 20986−20989.
72. Daoud, R., Julien, M., Gros, P., and Georges, E. (2001) *J. Biol. Chem. 276*, 12324−12330.
73. Ramachandra, M., Ambudkar, S. V., Chen, D., Hrycyna, C. A., Dey, S., Gottesman, M. M., and Pastan, I. (1998) *Biochemistry 37*, 5010−5019.
74. Taguchi, Y., Kino, K., Morishima, M., Komano, T., Kane, S. E., and Ueda, K. (1997) *Biochemistry 36*, 8883−8889.
75. Chang, G., and Roth, C. B. (2001) *Science 293*, 1793−1800.

BI034462B